Low-Salinity Chase Waterfloods Improve Performance of Cr(III)-Acetate Hydrolyzed Polyacrylamide Gel in Fractured Cores

Bergit Brattekås, The National IOR Centre of Norway, University of Stavanger; **Arne Graue,** University of Bergen; and **Randall S. Seright,** New Mexico Petroleum Recovery Research Center

Summary

Polymer gels are frequently applied for conformance improvement in fractured reservoirs, where fluid channeling through fractures limits the success of waterflooding. Placement of polymer gel in fractures reduces fracture conductivity, thus increasing pressure gradients across matrix blocks during chase floods. A gel-filled fracture is reopened to fluid flow if the injection pressure during chase floods exceeds the gel-rupture pressure; thus, channeling through the fractures resumes. The success of a polymer-gel treatment, therefore, depends on the rupture pressure.

Salinity differences between the gel network and surrounding water phase are known causes of gel swelling (e.g., observed in recent work on preformed particle gels). Gel swelling and its effect on fluid flow have, however, been less studied in conjunction with conventional polymer gels. By use of corefloods, this work demonstrates that low-salinity water can swell conventional Cr(III)-acetate hydrolyzed polyacrylamide (HPAM) gels, thereby significantly improving gel-blocking performance after gel rupture.

Formed polymer gel was placed in fractured core plugs, and chase waterfloods were performed using four different brine compositions, of which three were low-salinity brines. The fluid flow rates through the matrix and differential pressures across the matrix and fracture were measured and shown to increase with decreasing salinity in the injected water phase. In some cores, the fractures were reblocked during low-salinity waterfloods, and gel-blocking capacity was increased above the initial level. Low-salinity water subsequently flooded the matrix during chase floods, which provided additional benefits to the waterflood. The improved blocking capacity of the gel was caused by a difference in salinity between the gel and injected water phase, which induced gel swelling. The results were reproducible through several experiments, and stable for long periods of time in both sandstone and carbonate outcrop core materials. Combining polymer gel placement in fractures with low-salinity chase floods is a promising approach in integrated enhanced oil recovery (IEOR).

Introduction

Polymer gel networks and their behavior have been studied in conjunction with a wide range of applications and industries, including medicine (tissue engineering, artificial muscles, sustained-release drug-delivery systems), consumer products (disposable absorbent diapers, contact lenses, rubber, clothing, and textiles), and the oil-and-gas industry, and have been subjects of interest for decades. The behavior of polymeric gel under a variety of conditions is, therefore, fairly well-understood, and was shown to depend on properties of the gel itself as well as external conditions.

In the oil-and-gas industry, one can use polymer gels for conformance control in fractured or heterogeneous reservoirs: Gel is then injected to reside in a high-permeability zone or fracture to divert flow during chase floods. Gel is often placed in a reservoir as a low-viscosity gelant (a solution containing all gel components that have not yet chemically reacted). Depending on composition and conditions, the formulation may mature during pumping close to the wellbore; thus, preformed, high-viscosity gel extrudes through fractures during the placement process. Both placement methods were studied in detail, and are well-understood in water-saturated porous media (Liang et al. 1993; Seright 1995, 2001, 2003a; Ganguly et al. 2002; McCool et al. 2009). Because of its highly viscous and rigid nature once it has matured, polymer gel can efficiently reduce flow in fractures, and injected chase fluids (water, gas, EOR chemicals) may be diverted into rock matrix that has not been flooded previously. The success of a chase flood depends mostly on the gel's ability to block high-permeability anomalies (i.e., fractures), and therefore relies on gel properties during subsequent flooding. The gel's mechanical strength dictates the pressure that the gel is able to withstand during chase floods. The rupture pressure of the gel (the pressure at which the gel "breaks" and allows fluids to pass through it) is of special importance; a gel that has ruptured has a decreased blocking capacity and permits a higher degree of fracture flow compared with the intact gel originally in place (Ganguly et al. 2002; Seright 2003b; Wilton and Asghari 2007; Brattekås et al. 2015). A gel's ability to reduce conductivity in fractures is directly linked to its mechanical strength, but also relies on the gel's ability to completely occupy a fracture volume (FV).

Changes in the external conditions around a polymer gel network may alter the gel volume and, hence, affect the blocking capacity of gel residing in a fracture, by controlling the fraction of the FV that is filled by gel at all times, and are crucial to the success of conformance improvement in fractured reservoirs. The swelling and shrinking behavior of formed polymer gel networks is well-known, and has been attributed to changes in external conditions such as temperature, solvent composition, ionic strength, and external electric field (Horkay et al. 2000). The volumetric behavior of a polymer gel after placement in a reservoir, and particularly during chase-flood injections, is important (Young et al. 1989), mostly because polymer properties are known to change when in contact with reservoir fluids. For polymer solutions, viscosity and long-term stability have been observed to decrease with increasing salinity in the surrounding brine phase (Akstinat 1980; Uhl et al. 1995; Choi et al. 2010; Wu et al. 2012).

For crosslinked polymer solutions, numerous studies have shown that one can attribute volumetric changes in a gel after placement in a reservoir to *syneresis* (Vossoughi 2000; Romero-Zeron et al. 2008), in which solvent is expulsed from the gel network, or *dehydration*, either from imposing an external pressure gradient on the gel network (Al-Sharji et al. 1999; Krishnan et al. 2000; Wilton and Asghari 2007) or caused by capillary spontaneous imbibition of solvent from the gel into an oil-saturated adjacent porous rock (Brattekås et al. 2014). Recent works have also concentrated on the swelling and shrinking behavior of polymer gels caused by contrasts in salinity or pH between the gel solvent and formation fluids, which influence the osmotic pressure

This paper (SPE 173749) was accepted for presentation at the SPE International Symposium on Oilfield Chemistry, The Woodlands, Texas, USA, 13–15 April 2015, and revised for publication. Original manuscript received for review 22 January 2015. Revised manuscript received for review 21 September 2015. Paper peer approved 24 September 2015.

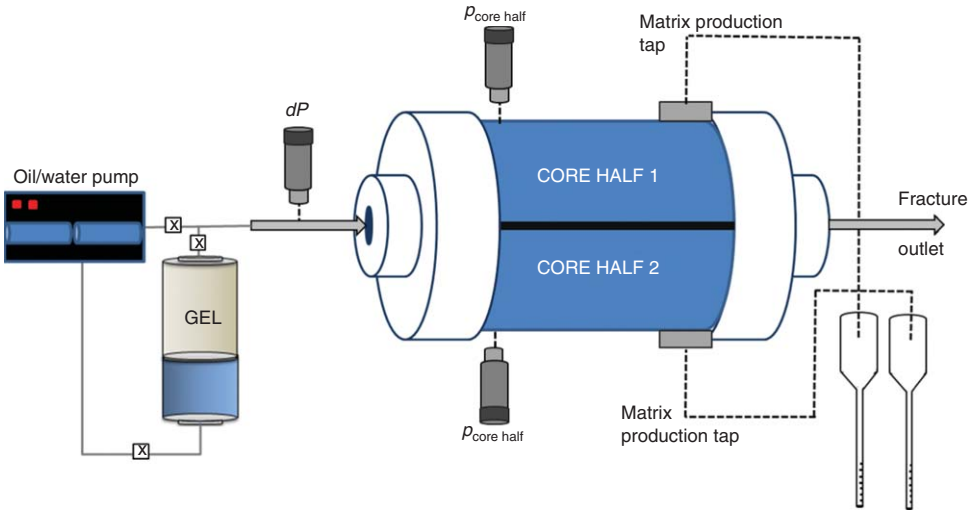

Fig. 1—Schematic of the fractured core plug and experimental setup.

balance between a polymer gel network and its surroundings. The effect of salinity contrasts has often been demonstrated in studies on preformed-particle-gel (PPG) networks, which show different gel-swelling behavior in brines of different salinity (Bai et al. 2007; Zhang and Bai 2011). Experimental studies performed on bulk volumes of gel demonstrated that volumetric changes in a gel network may occur if the salinity or pH of a contacting aqueous phase differs from the gel solvent (Aalaie et al. 2009; Tu and Wisup 2011). Tu and Wisup (2011) indicated that volumetric swelling of the gel could improve conformance when the salinity of the formation brine was lower than that of the gel solvent. Aalaie et al. (2009) described the phenomenon as "undesired," mainly due to the presence of mono- and multivalent cations in oil-reservoir water, which may cause deswelling (shrinking) of the gel network. Few works have yet focused on swelling effects caused by salinity contrasts between injected water and gel solvent during chase waterflooding in gel-filled fracture networks.

This work sought to investigate whether gel swelling caused by salinity contrasts between the gel solvent and injected water phase could improve conformance control in open fractures, and could restore matrix flow after gel rupture. Experiments were performed with an HPAM Cr(III)-acetate gel with a high-salinity solvent that was placed in open fractures through sandstone and carbonate core plugs. The gel rapidly ruptured during chase waterflooding, and most of the injected water was produced through the fracture. Low-salinity waterfloods, applying three different brine compositions, were thereafter performed. We found that a reduced salinity in the injected water phase with respect to the gel solvent improved the blocking performance of the gel: (1) injection pressures increased during low-salinity floods, and exceeded the initial gel-rupture pressure in all experiments and (2) matrix production rates increased during low-salinity flooding, dependent on the salinity content of the injected water phase. The fracture was, in some core plugs, completely reblocked during low-salinity waterflooding. The swelling of the polymer gel network was reversible, and gel-blocking efficiency immediately decreased when water of the same composition as the gel solvent was injected.

Experiments

Core Preparation. Cylindrical outcrop core plugs were drilled out from larger slabs of Bentheimer sandstone (permeability, $K = 1.2$ D, and porosity, $\Phi = 23\%$) (Schutjens et al. 1995; Klein and Reuschle 2003) and Edwards limestone ($K = 3$ to 28 mD, and $\Phi = 16$ to 26%) (Tie 2006; Johannesen 2008), and cut longitudinally with a band saw, which created smooth fractures. Core and fracture surfaces were washed with tap water, and the core plugs were dried for one week, first at room temperature and thereafter at an elevated temperature of 60 °C. Fractured core plugs were assembled by placing a polyoxymethylene (POM) spacer between two core halves, creating a 1-mm fracture aperture with a calculated permeability of approximately 8.4×10^4 D (Witherspoon et al. 1980). The fractured cores were coated in several layers of epoxy, and facilitated one common inlet for flow (both matrix and fracture) and three outlets (one for each matrix core half and one fracture outlet). The fracture outlet consisted of a POM end piece and a Swagelok fitting, measuring 2 cm in total with a 3.2-mm ID. The fracture outlet was open during most waterfloods (no additional tubing). Pressure taps were drilled into each matrix core half, approximately 1 cm from the inlet end face. The core and experimental setup can be seen in **Fig. 1.** Five fractured core plugs were used in this study: two consisting of Edwards limestone (Core 1_EDW and Core 2_EDW), one consisting of Bentheimer sandstone (Core 1_BS), and two composite core plugs in which a sandstone and a limestone core half were assembled and separated by the open fracture (Core 1_EDW_BS and Core 2_EDW_BS). The cores were saturated directly by mineral oil (*n*-decane) under vacuum, and porosity was calculated from weight measurements. The permeability of the cores could not be explicitly measured because of the experimental setup, but a relative measure for core-matrix conductivity

Core ID	Length (cm)	Diameter (cm)	Pore Volume (cm^3)	Porosity (%)	Conductivity Contrast	Gel Injected (PV)	Fracture Volume FV (cm^3)	Gel Breakthrough (FV)
1_EDW_BS	7.34	5.03	37.25	28.14*	48.4	21.3	3.7	5.4
2_EDW_BS	7.25	5.02	39.08	29.79*	42.9	20.3	3.6	3.0
1_EDW	7.18	4.78	33.36	25.89	None	23.8	3.4	4.4
1_BS	6.94	5.15	35.99	24.89	None	22.1	3.6	4.4
2_EDW	14.74	4.89	67.66	24.50	None	11.7	7.2	1.6

*mean value

Table 1—Core-plug properties.

	Formation Water (FW)	*LowSal1*	*LowSal2*	*LowSal3*
NaCl (g/L)	40	1	0.5	0
$MgCl_2$*6 H_2O (g/L)	34	0	0	0
$CaCl_2$*2 H_2O (g/L)	5	0	0	0
Brine salinity (ppm)	79,170	1,000	500	0

Table 2—Brine compositions, used for gel preparation and chase waterflooding.

Fluid	Density (g/cm^3)	Viscosity (10^{-3} Pa·s) at 20°C	Composition
n-Decane	0.73	0.92	Isotopic purity >95%
HPAM Gel	~1.048	~2*10^6 after gelation*	0.5% HPAM 0.0417% Cr(III)-Acetate FW

*Liu and Seright (2001)

Table 3—Fluid properties of *n*-decane and bulk HPAM gel (mature, as used in the experiments).

was found by flooding *n*-decane from the inlet and through each of the matrix outlets separately while measuring the absolute and in-situ pressure drops. An overview of the fractured core plugs and their properties can be found in **Table 1.**

Experimental Schedule. The experimental schedule consisted of two separate steps: (1) a gel placement and (2) a subsequent waterflood. Through both experimental steps, the pressures across the core and in each core half were recorded, and fluid production rates from the matrix and fracture outlets were logged.

Gel Placement. *Gel Preparation.* The polymer gel used in the experiments was a commercially available HPAM crosslinked by Cr(III)-acetate. Gel was prepared by mixing polymer in brine at 5,000-ppm concentration. 417-ppm Cr(III)-acetate was thereafter added to the polymer solution, and the gelant (non-crosslinked gel solution) was aged in an accumulator at 41 °C for 24 hours (five times the gelation time). Gel injections and subsequent waterfloods were performed at ambient conditions, and the mature gel was allowed to cool down to room temperature before gel injection started. The gel solvent was high-salinity formation water (FW) from a North Sea chalk reservoir **(Table 2).**

Gel Injection. Mature gel was injected into the fractured cores at a constant injection rate of 200 mL/h. During mature gel injection, the gel itself will only progress through the open fracture, but gel solvent may leave the gel and flood the matrix during a leakoff process (Seright 2003a). Volumetric recordings of fluid production from the matrix and fracture outlets were performed, and gel breakthrough at the fracture outlet was recorded (tabulated in Table 1). A total of 800 mL of gel was injected into each core. After gel placement, the cores were shut in for 24 hours with all inlets and outlets closed.

Waterflooding. Waterfloods were performed to measure the blocking capacity of the gel residing in the open fractures, and the blocking-capacity dependency on the chase-water composition. Matrix outlets were open during waterflooding, and fluid production from each core half, and from the fracture outlet, was recorded. The main purpose of initial waterflooding was to rupture the gel in the fracture and measure the rupture pressure, P_R. During continued waterflooding after gel rupture, the majority of injected water flows through the fracture without entering the matrix to displace oil. We investigated whether salinity differences between low-salinity injection water and higher salinity gel solvent could cause sufficient swelling of the gel in place to improve conformance control in the wide fractures and to restore matrix flow. Different brine compositions were used for waterflooding, including FW and three different low-salinity brines; they are listed in Table 2. The oil and bulk gel properties are given in **Table 3.** The waterflood schedule was specific for each fractured core **(Table 4),** in which injected water salinity was either varied throughout the experiment or kept constant at a low value. The pressures across the fractured core plugs, in-situ matrix pressures, and volumetric recordings of fluid production from the matrix and fracture outlets were measured during waterfloods. Pressures and production rates combined gave insight to gel-blocking capacity and changes in gel performance caused by low salinity-induced gel swelling.

A low injection rate of 6 mL/h was used during most chase waterfloods (Table 4), and was chosen to maintain a comparable flow rate in the matrix throughout all the experimental steps. Although an injection rate of 200 mL/h was used for gel placement, this rate is only descriptive of gel flow in the fracture. The solvent leakoff rate from the gel to the matrix was measured to be quite low (<20 mL/h). The water injection rate was changed in one core (1_EDW_BS) during low-salinity waterflooding before gel swelling (as shown later in Fig. 6). The results did not suggest quantitative differences between gel behavior during short-term high-salinity (Brattekås et al. 2015) and low-salinity waterflooding.

Results

Gel Placement. The first experimental step was gel placement, in which mature gel was injected through each fractured core plug at a constant injection rate of 200 mL/h (equivalent to 305 to 330 ft/D when all flow is confined to the fracture). Mature gel is confined to fractures during injection; however, solvent may leave the gel in the fracture and leak off into the matrix (Seright 2003a). This behavior causes the gel in the fracture to concentrate and become more resistant to applied pressure gradients, and is an important distinction from in-situ gelation systems, in which the gel concentration in the fracture and adjacent matrix is uniform after placement.

Core ID	Injection Rate (cm^3/h)	Duration (hours)	Brine-Injection Sequence				
1_EDW_BS	6 – 499	44	(1)*LowSal3*				
2_EDW_BS	6 (const)	886	(1)FW	(2)*LowSal1*	(3)*LowSal2*	(4)*LowSal3*	(5)FW
1_EDW	6 (const)	166	(1)FW	(2)*LowSal1*	(3)*LowSal2*	(4)*LowSal3*	(5)FW
1_BS	6 (const)	210	(1)FW	(2)*LowSal1*	(3)*LowSal2*	(4)*LowSal3*	(5)FW
2_EDW	6 (const)	3,979	(1)*LowSal3*				

Table 4—Waterflood schedules for each core.

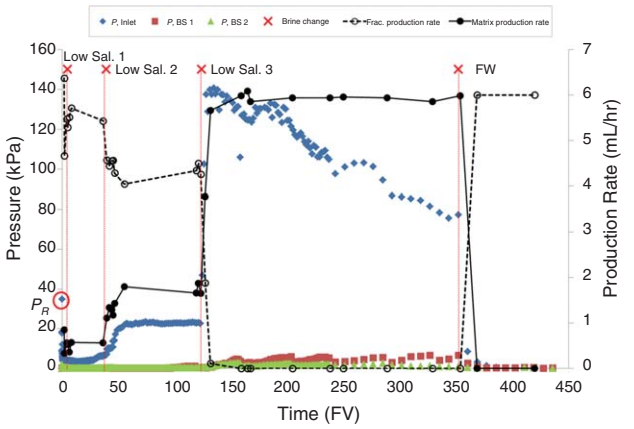

Fig. 2—Measured differential pressures (left *y*-axis) and production rates (right *y*-axis) across the fracture and matrix core halves during sequential water injection in Core 1_BS. Changes in brine composition are denoted by red crosses and vertical lines intersecting the *x*-axis.

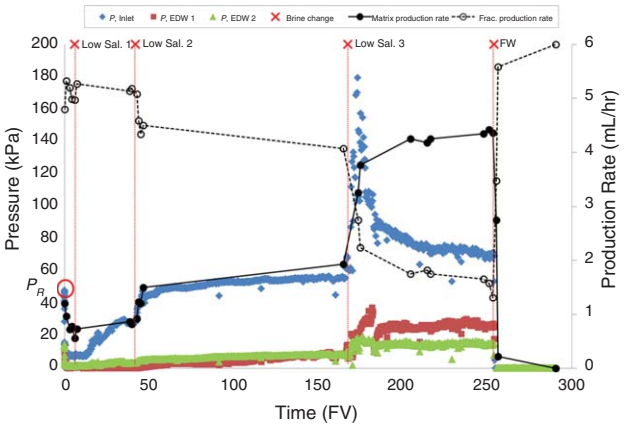

Fig. 3—Measured differential pressures (left *y*-axis) and production rates (right *y*-axis) across the fracture and matrix core halves during sequential water injection in Core 1_EDW. Changes in brine composition are denoted by red crosses and vertical lines intersecting the *x*-axis.

The behavior of the gel during extrusion through a fracture, specifically the extent to which solvent leaves the gel, has important implications for gel-blocking efficiency during chase floods (Brattekås et al. 2013, 2015), because solvent leakoff tells us something about the gel's tendency to concentrate and form wormholes. Lower leakoff rates than Seright's filter-cake model (Seright 2003a) were observed during gel extrusion in all core plugs, and the solvent flow rate in the matrix was measured to be 20 mL/h and below. Still, several pore volumes (PVs) of water left the gel during extrusion and reduced the matrix saturation from 100% oil saturation to the residual oil saturation (ROS) (S_{or}) within two hours of gel-injection initiation. At S_{or}, shrinkage of the gel because of capillary spontaneous imbibition of gel solvent will not occur, and the gel volume remained stable during the 24-hour shut-in period between gel placement and waterflooding (Brattekås et al. 2014). Gel breakthrough occurred between 1.6 and 5.5 FV of gel injected (tabulated in Table 1). We assume that fresh gel extruded through concentrated gel in wormholes for the remaining injection period (ranging from 110 to 220 FV).

Waterflooding. The outcrop core plugs used in this work were strongly water-wet, and wettability will not be altered when the cores are saturated by pure mineral oil (e.g., *n*-decane). Waterfloods were initiated at S_{or}; hence, additional recovery of oil during waterflooding was not expected or recorded during these experiments. In systems at less water-wet conditions, increased oil recovery can occur during low-salinity waterflooding (Morrow and Buckley 2011), and is an added benefit to the improved blocking capacities of the gel that were observed and quantified in the following.

Varying the Salinity of the Injected Water Phase. In three fractured core plugs (1_EDW, 1_BS, and 2_EDW_BS), brine salinity was varied during waterflooding. The results are shown in **Fig. 2** (Core 1_BS), **Fig. 3** (Core 1_EDW), and in **Figs. 4 and 5** (Core 2_EDW_BS).

High-Salinity FW. High-salinity FW (with the same composition as the gel solvent) was first injected at 6 mL/h, during which initial gel rupture was achieved, and the rupture pressure (P_R) was measured. P_R was measured with both the matrix and fracture outlets open and was recorded at 5.03 kPa/cm (Core 1_EDW), 6.44 kPa/cm (Core 1_BS), and 3.10 kPa/cm (Core 2_EDW_BS). The recorded values were slightly higher than previously measured rupture pressures after gel placement at the same gel-injection rate (Brattekås et al. 2015); a deviation probably caused by the experimental design (open matrix outlets in this work compared with only the fracture outlet open in previous work). The rupture

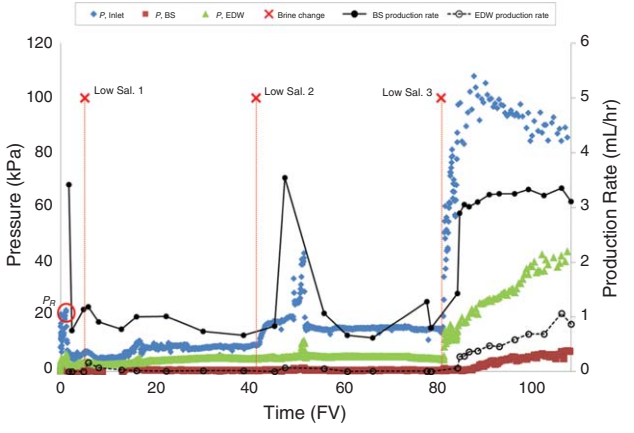

Fig. 4—Measured differential pressures (left *y*-axis) and production rates (right *y*-axis) across the fracture and matrix core halves during the start of sequential water injection in Core 2_EDW_BS. Changes in brine composition are denoted by red crosses and vertical lines intersecting the *x*-axis.

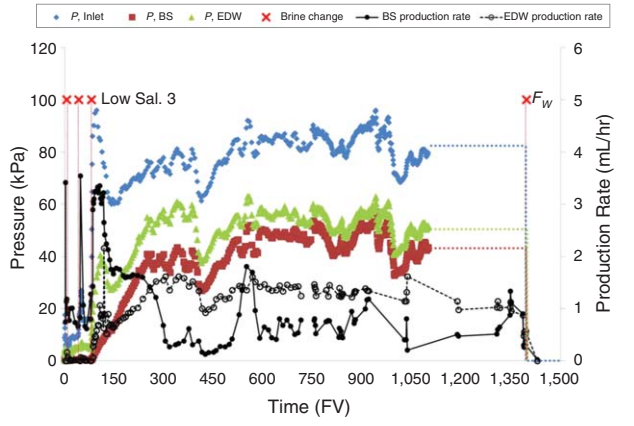

Fig. 5—Measured differential pressures (left *y*-axis) and production rates (right *y*-axis) across the fracture and matrix core halves for the duration of water injection in Core 2_EDW_BS. Changes in brine composition are denoted by red crosses and vertical lines intersecting the *x*-axis. The pressure logging tool failed after $t = 1{,}100$ FV water injected. The pressure profiles for the remainder of the experiment were recorded by visual inspection, indicated in the dotted blue, green, and red lines in the figure.

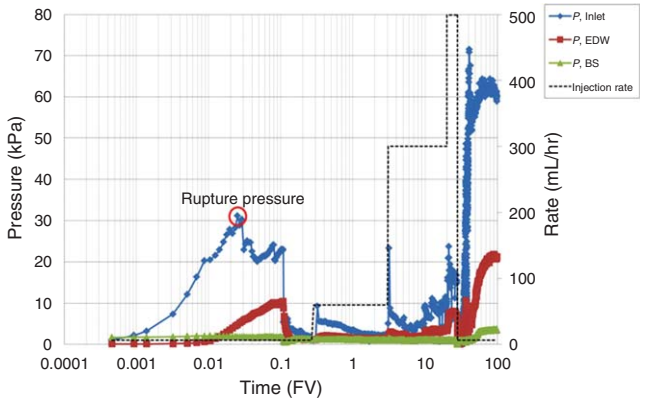

Fig. 6—Measured differential pressures across the fracture and matrix core halves during low-salinity water injection in Core 1_EDW_BS. The *x*-axis is given in logarithmic scale, to better see the results from short-term waterflooding ($t = 0$ to 28 FV injected).

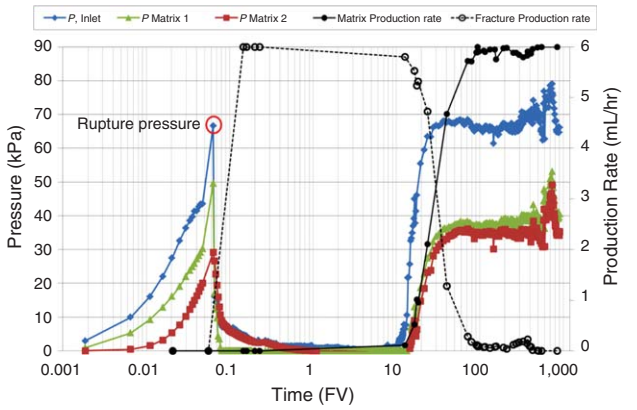

Fig. 7—Measured differential pressures (left *y*-axis) and production rates (right *y*-axis) across the fracture and matrix core halves during low-salinity waterflooding of Core 2_EDW. The *x*-axis is given in a logarithmic scale for improved viewing of early waterflood characteristics.

pressures are indicated by red circles in the figures. After gel rupture, the pressure gradients across the core and in both core halves were allowed to stabilize before altering the composition of the injected water phase. The salinity content was thereafter reduced stepwise throughout waterflooding, first applying *LowSal1* water. *LowSal1* had the highest salt content of the three low-salinity water compositions, at 1,000-ppm NaCl. During *LowSal1* injection, a slight increase in injection pressure occurred in all three cores, being most prominent in Core 1_EDW. A corresponding, minor drop in fracture-production rate was also observed. After approximately 10 PV *LowSal1* injected, the systems stabilized, and pressures and production rates remained close to constant until more than 40 PV total of *LowSal1* water was injected. The salinity of the injected water phase was reduced further: shortly after *LowSal2* initiation, a more-prominent increase in pressures and matrix production rates was observed in all cores. In Cores 1_BS and 1_EDW, an abrupt drop in fracture production rate occurred, indicating that the gel-blocking capacity increases as the gel swells and fills a larger volumetric section of the fracture. Further decrease in injected water-phase salinity, using the *LowSal3* water composition, caused further swelling of the gel, and an abrupt increase in injection pressure and matrix production rate occurred. In all three cores, the injection pressure increased up to more than three times the initial gel-rupture pressure. The fracture production rates dropped abruptly as the injection pressure increased: in Cores 1_EDW and 2_EDW_BS, approximately 33% of the fluids were transported through the fracture after the system had stabilized during *LowSal3* waterflooding, while the remaining 67% of water flooded the matrix. In Core 1_BS, the fracture was efficiently sealed off during *LowSal3* water injection, and all fluids were produced through the matrix. This indicates that injection of low-salinity water not only improves gel performance after rupture compared with injection of higher salinity water (e.g., seawater or FW), but also greatly enhances gel performance above the initial level.

In Core 2_EDW_BS, more than 1,200 FV of *LowSal3* were injected to investigate the long-term stability of the gel-blocking ability. The pressure gradients and production rates remained stable for this period, although with small fluctuations, and loss of gel-blocking capacity with time and high-water throughput was not indicated. A decreasing trend in injection pressure was observed during *LowSal3* waterflooding of Core 1_EDW and Core 1_BS. The decrease in pressure had no apparent effect on the matrix and fracture production rates, nor on the measured in-situ pressures, and was probably caused by erosion of the gel layer between the inlet injection point and the matrix: This will aid water to more efficiently enter and flood the matrix, without influencing the gel-blocking capacity in the fracture.

The final step in the waterfloods in this section was a second injection of high-salinity FW, to investigate whether improvement in blocking capacity was reversible. When FW entered the fractured cores, injection pressures immediately decreased to a low value, and fluid production through the fractures commenced. Less than 10 FV of FW was injected before the effects of low-salinity flooding on the gel were completely eliminated, and the gel-blocking capacity was minimized. The gel swelling caused by salinity differences between the gel solvent and injected water phase therefore appears to be reversible, and gel-swelling effects, which cause improved fracture blocking, depend on continuous injection of water with a lower salinity than the gel solvent.

Direct Waterflooding by Low-Salinity Water. In Core 1_EDW_BS and Core 2_EDW, waterflooding after gel placement was performed with the *LowSal3* brine composition (distilled water) only; thus, the injected water phase differed in composition from the gel solvent for the duration of waterflooding. The results are shown in **Fig. 6** (Core 1_EDW_BS) and **Fig. 7** (Core 2_EDW). The rupture pressures were measured at 4.3 kPa/cm and 4.8 kPa/cm, respectively, which are comparable to the measured rupture pressures after gel placement in the previous section.

In Core 1_EDW_BS, water injection continued after gel rupture with varying injection rates to measure the gel-blocking characteristics. The pressure trends measured at the inlet and in the respective core halves are shown in Fig. 6. The gel ruptured shortly after waterflood initiation and water production from the fracture outlet was observed. The differential pressure rapidly decreased when the rupture pressure was reached, and all production of fluids was subsequently through the fracture. By varying the water-injection rate, peaks in pressure were seen, followed by swift pressure drops. This is a characteristic behavior of the gel when placed in open fractures, owing to the erosion of wormholes, and is expected at higher injection rates (Brattekås et al. 2015). Reducing the injection rate to 6 mL/h (comparable to the previous section) resulted in a reduction of the pressures across the core and in both core halves to close to zero. So far, the results did not suggest quantitative differences between gel behavior during short-term high-salinity (Brattekås et al. 2015) and low-salinity waterflooding. *LowSal3* injection continued at 6 mL/h for 100 FV of water injected, corresponding to an injection time of approximately 44 hours. Between $t = 28$ to 32 FV, pressures remained low, and water production was only observed through the fracture. From $t = 32$ FV injected ($\approx$4.5 hours), the pressure drop across the core increased, as did the pressure in both core halves. From $t = 60$ FV injected ($t \approx 20$ hours), the pressures remained constant at a value twice as high as the initially measured rupture pressure. The matrix production rate in this time period totaled 2.8 mL/h, which is slightly less than 50% of the total production rate: The remaining water volume was produced through the fracture.

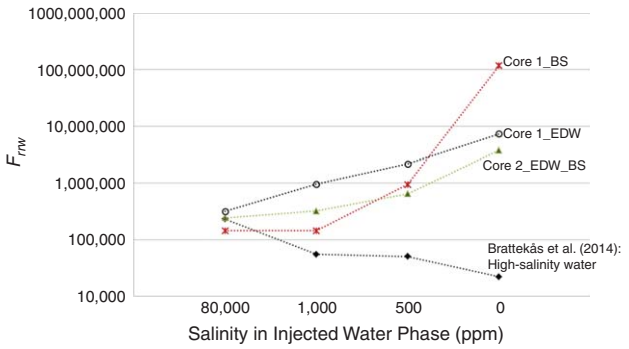

Fig. 8—The F_{rrw} measured in the fracture during waterflooding at 6 cm³/h as a function of decreasing salinity (Core 1_BS, Core 1_EDW, and Core 2_EDW_BS) and increasing time after gel rupture (all cores). In conventional gel behavior, in which there is no salinity contrast between gel solvent and injection water, F_{rrw} decreases with water throughput. Core 3 from Brattekås et al. (2015) is included in the figure as an example of conventional gel behavior in a similar system.

In Core 2_EDW, the injection rate was not varied, and water was injected at a constant injection rate of 6 mL/h for more than 1,000 hours. The results are shown in Fig. 7. The rupture pressure was reached shortly after the start of water injection, after which the pressures across the core and in both core halves decreased and the fracture production rate abruptly rose to 6 mL/h (all injected fluids flow through the fracture). After an incubation period of approximately 8 FV ($t \approx 12$ hours), during which *LowSal3* was continuously injected, the pressures increased to the level of the initial gel-rupture pressure and remained constant for a prolonged period of time (>1,000 FV injected). The matrix production rate increased alongside the pressure profiles: A minor increase in matrix production was observed during the incubation time, with a steep increase from $t = 12.6$ to 93.8 FV. The matrix production rate remained stable from $t = 94$ FV injected, at which point, the fracture was efficiently sealed off by gel, and all fluids were produced through the matrix. The pressures and matrix-production rates remained stable at high levels for a long time period ($t > 1{,}000$ FV injected); thus, the improved blocking ability of the gel residing in the fracture was continuous and stable.

Because of the strongly water-wet characteristics of the core material, additional oil recovery during waterflooding was not observed in the previous experiments. However, during long-term *LowSal3* waterflooding of 2_EDW, a few oil drops were produced alongside rock particles: This suggests that the oil drops were formerly capillary trapped, and produced as a result of the dissolution of core material following the collapse of pores and throats, resulting from the injection of several hundred PVs of water. In field applications, in which the matrix-block volume far surpasses the FV, gel placement alone will not significantly contribute to oil recovery, and the potential for EOR during low-salinity chase floods is higher.

Discussion

The increase of fracture-flow capacity caused by gel rupture and dehydration during chase waterflooding is generally expected to be irreversible. However, gel treatments may still reduce fracture flow after rupture because of the inherent elasticity of the gel, which allows wormholes to collapse and reopen depending on the applied differential pressure (Wilton and Asghari 2007; Brattekås et al. 2015). Previous observations indicate that the rupture pressure is the ultimate pressure achievable during chase waterfloods and that fluid flow through fractures after the gel ruptures cannot be easily reduced. Our experimental work shows how the blocking capacity of a ruptured gel treatment may be improved, and partly controlled, by varying the salinity of the injected water relative to the gel solvent. **Fig. 8** shows the average residual resistance factor (F_{rrw}) in the fracture when injected water salinity was reduced during waterflooding. The F_{rrw} is the ratio of initial to post-gel treatment fracture conductivity, and provides a measure of the permeability reduction achieved by the gel. Each F_{rrw} was calculated from the pressure drop at 6 mL/h for each brine composition during waterflooding of Core 1_EDW, Core 1_BS, and Core 2_EDW_BS (in which salinity was reduced during waterflooding). Data from Brattekås et al. (2015) are also included for comparison, and give insight to conventional behavior of gel during waterflooding in which the F_{rrw} is usually observed to decrease. In Core 1_EDW, Core 2_EDW_BS, and Core 1_BS, we observed that each F_{rrw} increased when low-salinity waterfloods were implemented after gel rupture. Average F_{rrw} values measured during *LowSal3* waterflooding were 330 and 169 times higher than during high-salinity FW injection in Core 1_EDW and Core 2_EDW_BS, respectively. In Core 1_BS, average F_{rrw} was almost 5,300 times higher, and converged toward infinity because the fracture was completely reblocked (zero conductivity) during the *LowSal3* waterflood. The F_{rrw} values were not consistent among the cores because of differences in core material and solvent leakoff during gel placement. By decreasing the salinity content in the injected water phase relative to the gel-solvent, improved fracture-permeability reduction was achieved; thus, gel-blocking ability improved with water throughput in these experiments (Table 4). When water with the same composition as the gel solvent (no salinity contrast) was injected, the gel-placement method and applied differential pressure controlled the rate of F_{rrw} decrease (Brattekås et al. 2015).

The work presented in this paper shows, for the first time, significant improvement in gel-blocking ability during long-term waterflooding of fractured cores, caused by salinity differences between the gel solvent and injected low-salinity water phase. Note that, theoretically, the injected water-phase salinity does not have to be limited to low-salinity water (commonly, <2,000-ppm salinity content) to produce this effect: injected-water salinity may be reduced with respect to the gel solvent with the intention to improve gel-blocking capacity only. Gel of particularly high salinity may, in such scenarios, be placed in the reservoir. Although the added benefit of low-salinity flooding of the matrix will not be achieved, favorable effects may occur: (1) the gel may swell after contacting FW (if the salinity of the gel solvent exceeds FW salinity), which improves the gel-blocking ability before rupture, and (2) injection of seawater may induce the same gel swelling benefits that low-salinity waterflooding demonstrated in this study. One can argue that, in most polymer gel applications in fractured reservoirs, it is desirable to use a gel solvent similar to the FW composition to avoid reactions between the gel and FW during and after gel placement. FW in most reservoirs is saline, and commonly of high-salinity. Concerns about the long-term stability of polymer gels with high-salinity solvent has previously been addressed, and an increased degree of syneresis was pointed out as a good reason to stay below certain concentrations of mono- and multivalent cations in the gel solvent (Aalaie et al. 2009). Detailed studies of gel-solvent compositions and their effects on gel stability may therefore be required before field applications, as are experiments on reservoir conditions. However, the results presented in this paper are encouraging and show that (1) the short-term behavior of high-salinity gel, as used in this study, was comparable to gel containing 5% NaCl only, both during and after injection into an open fracture (Seright 2003a; Brattekås et al. 2015), (2) the experiments performed on Core 2_EDW and Core 2_EDW_BS demonstrated that the blocking capacity of high-salinity gel remained stable for more than 1,000 hours of low-salinity waterflooding, and (3) visual observations on bulk volumes of high-salinity gel did not suggest additional syneresis in the gel used in this study.

In our work, we injected gels that were formulated in relatively high-salinity water. One might ask, Why not inject a low-salinity gel in the beginning (because it is presumably stronger)? If a low-salinity gel is injected initially, relatively high pressure gradients could limit the distance of gel penetration into the fracture or fracture system. Further, once the gel is in place, contact with the high-salinity FW could shrink the gel—thereby opening a flow path through the fracture. By injecting a high-salinity gel, we

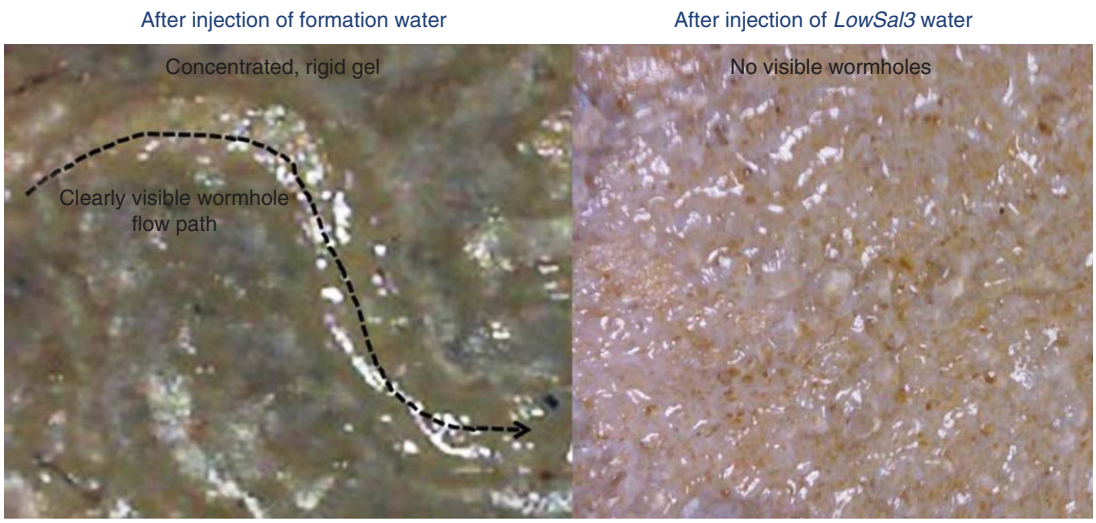

Fig. 9—Wormholes (left) were efficiently plugged by gel swelling during low-salinity water injection (right).

hope to maximize the distance of gel penetration into the fracture, and we allow enhanced reduction of fracture-flow capacity during subsequent injection of low-salinity water.

Mechanism Behind Improved Blocking. We advocate that the immobile gel "filter cake" that forms in the fracture during gel placement contains wormholes. The wormholes provide the rupture path for the injected water. After rupture, water flows in the wormholes, and the concentrated gel filling the fracture remains immobile. During low-salinity waterflooding, the gel surrounding the wormholes swells and constricts the water flow path. Evidence to support this mechanism can be seen in **Fig. 9.**

An alternative theory involves gel particles swelling and "lodging" flow paths. However, our results indicate that this is not the correct mechanism. Gel was produced from the fracture outlet only once—during initial waterflooding when the rupture pressure was measured. Gel was not observed coming out from the fracture outlet (in bulk or effluents) after gel rupture during long-term low-salinity waterflooding. Also, the fracture-blocking ability of the gel was immediately reduced when salinity was changed. No "new" rupture pressure was measured. This indicates that the gel in the fracture de-swells, and the wormholes were reopened to flow. If the increased blocking capacity was caused by gel particles lodging in the pathway, a reduction would be caused by (1) gel particles being flushed out of the fracture (i.e., a second "gel rupture") or (2) gel particles de-swelling, which relies on direct contact between the gel and high-salinity water phase (relies on the slow process of diffusion when the fracture is supposedly filled with low-salinity water at the given pressure). In either case, gel production from the fracture would occur.

Validity of Results on Field Scale. Our work has focused on one fracture width (1 mm) and a limited range of gel compositions. Of course, the efficiency of our proposed method may vary with higher fracture apertures and lower initial gel strength. Additional work is needed to establish whether our method has broad applicability. However, the experiments demonstrate that adjusting the injected water-phase salinity with respect to the gel solvent strongly influences gel-blocking ability. This subsection discusses properties that may be influential on the field scale.

Mature vs. Immature Gel. In our experiments, mature gel was injected to reduce flow in open fractures. Previous work demonstrated that mature gel only progresses through open fractures, and that its concentration and rigidity increase during extrusion because solvent leaves the gel in a leakoff process (Seright 1999; 2001; 2003a). Fresh gel flows through the concentrated gel in wormholes, which are believed to be the weakest part of the gel during chase floods, and likely where the gel ruptures. The occurrence of wormholes through concentrated gel is largely responsible for a gel's ability to significantly reduce flow after it ruptures, because injected fluids are contained in the narrow flow channels constituting the wormholes. Because the wormholes are quite narrow and the gel surrounding them is quite concentrated (as a result of dehydration during placement), mature gel responds quickly to low-salinity waterflooding after placement in a fracture, because a small degree of gel swelling may efficiently constrict a wormhole. In contrast, in fractures where gel was placed in its immature state, the aperture of the rupture path may be quite wide—both because the brine/gel mobility contrast was less and the gel was more pliable than the concentrated preformed gel. Consequently, less pronounced effects may be seen during low-salinity brine injection, because the gel must experience a higher degree of swelling to fill a comparable section of the fracture. Although a valid concern, our results to this point are reassuring: Injection pressures during low-salinity waterfloods were measured to be above the initial rupture pressures in all experiments, and frequently two to three times as high. These are significant effects, particularly for 1-mm wide fractures, and indicate that gel-blocking efficiency caused by gel swelling may also be significantly improved in fractures with wider rupture apertures, for example experienced after immature gel placement, or in wider fractures. The swelling properties of bulk-gel volumes will provide insight into this issue, and must therefore be included in future work. Because of the short inherent gelation time of this gel system (approximately 5 hours at 41 °C), mature gel propagates through fractures during most of the placement process in large-volume field applications.

Scaling. During waterflooding, nonuniform matrix production from the core halves, as well as differences in in-situ pressure profiles, were seen in most cores—both in cores that did not have an inherent conductivity contrast (Cores 1_EDW and 1_BS) and in cores in which the conductivity contrast between the core halves was measured to be between 40 and 50 (Core 1_EDW_BS and Core 2_EDW_BS). The distribution of flow through a core plug with an inherent conductivity contrast is dictated by Darcy's law and controlled by the differential pressure across the core halves: Fluid channeling through the pathway of highest conductivity (e.g., fracture or high-permeability rock) is expected. In our experiments, we often found that conductivity contrasts were reflected in in-situ pressure profiles, but not in the production rates. For example, in Core 2_EDW_BS (Figs. 4 and 5), the sandstone core half produced more than twice the fluids compared with the Edwards limestone core half during the first 120 FV of waterflooding, but during *LowSal3* injection, a shift in production

occurred, and the lower permeability limestone conducted the majority of fluid flow for the remaining 1,000 FV of waterflooding. Nonuniform fluid production from the core halves is believed to be caused by small-scale differences at the inlet end faces of the core halves, a result of: (1) differences in gel erosion during waterflooding or (2) disintegration of core material during low-salinity waterflooding, causing small particles to lodge in pore throats and change the flow pattern—and will not be prominent on field scale, where matrix blocks are significantly larger compared with the FV. The experiments performed in this study were carefully designed to measure properties of the gel and flow simultaneously. Consequently, the ratio of FV to PV is higher in these experiments (approximately 10% of the core PV) compared with fractured reservoirs (≈1% of the reservoir PV). We believe that, during field operations, pressure gradients during chase waterflooding will be controlled mainly by the matrix flow capacity and not dictated by the gel, as observed in our experiments, as long as the injection pressure is below the gel-rupture pressure. Injectivity issues caused by gel swelling are not expected. In our experiments, gel swelled to constrict the water flow paths in the fracture, and hence improved blocking ability, but gel was not observed to swell outside the boundary of the fracture and core end faces. Concerning injectivity, the gel strength is substantially less than that of rock. The intent during a gel treatment in a field application is to propagate the gel quite deeply into the fracture or fracture system. During water injection after a gel treatment, pressure gradients will allow water to tear through gel in the near-wellbore portion of the fracture—enough to achieve the desired injectivity. Intact gel farther away from the well will mitigate channeling through the remainder of the fracture.

An optimum injection sequence to enhance oil recovery was not suggested in this work. Our experiments showed that gel swelling caused by low-salinity waterflooding was reversible and only dependent on continuous injection of a given water composition—thus, gel de-swelled, and fracture production restarted when FW with the same composition as the gel solvent was injected. Because of the flexibility of this system, an ideal IEOR process may be determined for each reservoir, and is not dependent on the order of fluids injected.

Conclusions

- Low-salinity waterfloods of fractured core plugs in which mature gel was placed in fractures improved the blocking capacity of the gel.
- Gel-blocking capacity improved when the injected water salinity was reduced with respect to the gel solvent.
- When water with a salinity that was almost 80,000 ppm lower than the gel solvent was injected, the injection pressure increased to above the initially measured rupture pressure in all cores, frequently stabilizing at a value two to three times higher than the rupture pressure.
- The fractures were efficiently blocked because of gel swelling during low-salinity waterflooding. In some cores, fracture flow was completely inhibited, and fluid flow occurred only through the fracture-adjacent matrix.
- The blocking capacity achieved by injection of low-salinity water remained stable for long periods of time, provided that low-salinity water was continuously injected into the fractured cores.
- When gel solvent was injected into the fractured cores after low-salinity waterflooding, gel de-swelled, and the blocking characteristics were reduced to the original level.

Nomenclature

F_{rrw} = residual-resistance factor
P_R = gel-rupture pressure
S_{or} = ROS

Acknowledgments

The National IOR Centre of Norway acknowledges the Research Council of Norway and our industry partners: ConocoPhillips Skandinavia A/S, BP Norge A/S, Det Norske Oljeselskap A/S, Eni Norge A/S, Maersk Oil Norway A/S, DONG Energy A/S Denmark, Statoil Petroleum AS, GDF Suez E&P Norge A/S, Lundin Norway AS, Halliburton AS, Schlumberger Norge AS, and Wintershall Norge A/S for support.

References

Aalaie, J., Rahmatpour, A., and Vasheghani-Farahani, E. 2009. Rheological and Swelling Behavior of Semi-Interpenetrating Networks of Polyacrylamide and Scleroglucan. *Polym. Adv. Technol.* **20:** 1102–1106. http://dx.doi.org/10.1002/pat.1369.

Akstinat, M. H. 1980. Polymers for Enhanced Oil Recovery in Reservoirs of Extremely High Salinities and High Temperatures. Presented at the SPE Oilfield and Geothermal Chemistry Symposium, Stanford, California, USA, 28–30 May. SPE-8979-MS. http://dx.doi.org/10.2118/8979-MS.

Al-Sharji, H. H., Grattoni, C. A., Dawe, R. A. et al. 1999. Pore-Scale Study of the Flow of Oil and Water Through Polymer Gels. Presented at the SPE Annual Technical Conference and Exhibition. Houston, USA, 3–6 October. SPE-56738-MS. http://dx.doi.org/10.2118/56738-MS.

Bai, B. J., Li, L. X., Liu, Y. Z. et al. 2007. Preformed Particle Gel for Conformance Control: Factors Affecting Its Properties and Applications. *SPE Res Eval & Eng* **10** (4): 415–422. SPE-89389-PA. http://dx.doi.org/10.2118/89389-PA.

Brattekås, B., Haugen, Å., Ersland, G. et al. 2013. Fracture Mobility Control by Polymer Gel- Integrated EOR in Fractured, Oil-Wet Carbonate Rocks. Presented at the EAGE Annual Conference and Exhibition Incorporating SPE Europec, London, 10–13 June. SPE-164906-MS. http://dx.doi.org/10.2118/164906-MS.

Brattekås, B., Haugen, Å., Graue, A. et al. 2014. Gel Dehydration by Spontaneous Imbibition of Brine From Aged Polymer Gel. *SPE J.* **19** (1): 122–134. SPE-153118-PA. http://dx.doi.org/10.2118/153118-PA.

Brattekås, B., Pedersen, S. G., Nistov, H. T., et al. 2015. Washout of Cr(III)-Acetate-HPAM Gels From Fractures: Effect of Gel State During Placement. *SPE Production & Operations* **30** (02): 99–109.

Choi, S. K., Sharma, M. M., Bryant, S. et al. 2010. pH-Sensitive Polymers for Novel Conformance-Control and Polymer-Flood Applications. *SPE Res Eval & Eng* **13** (6): 926–939. SPE-121686-PA. http://dx.doi.org/10.2118/121686-PA.

Ganguly, S., Willhite, G. P., Green, D. W. et al. 2002. The Effect of Fluid Leakoff on Gel Placement and Gel Stability in Fractures. *SPE J.* **7** (3): 309–315. SPE-79402-PA. http://dx.doi.org/10.2118/79402-PA.

Horkay, F., Tasaki, I., and Basser, P. J. 2000. Osmotic Swelling of Polyacrylate Hydrogels in Physiological Salt Solutions. *Biomacromolecules* **1:** 84–90. http://dx.doi.org/10.1021/bm9905031.

Johannesen, E. B. 2008. *NMR Characterization of Wettability and How It Impacts Oil Recovery in Chalk*. PhD thesis, 71, Department of Physics and Technology, Bergen, University of Bergen.

Klein, E. and Reuschle, T. 2003. A Model for the Mechanical Behaviour of Bentheim Sandstone. *Pure Applied Geophysics* **160:** 833–849. http://dx.doi.org/10.1007/PL00012568.

Krishnan, P., Asghari, K., Willhite, G. P. et al. 2000. Dehydration and Permeability of Gels Used in In-Situ Permeability Modification Treatments. Presented at the SPE/DOE Improved Oil Recovery Symposium, Tulsa, USA, 3–5 April. SPE-59347-MS. http://dx.doi.org/10.2118/59347-MS.

Liang, J.-T., Lee, R. L., and Seright, R. S. 1993. Gel Placement in Production Wells. *SPE Prod & Fac* **8:** 276–284. SPE-2021-PA. http://dx.doi.org/10.2118/2021-PA.

Liu, J. and Seright, R. S. 2001. Rheology of Gels Used for Conformance Control in Fractures. *SPE J.* **6** (2): 120–125. SPE-70810-PA. http://dx.doi.org/10.2118/70810-PA.

McCool, C. S., Li, X., and Wilhite, G. P. 2009. Flow of a Polyacrylamide/Chromium Acetate System in a Long Conduit. *SPE J.* **14** (1): 54–66. SPE-106059-PA. http://dx.doi.org/10.2118/106059-PA.

Morrow, N. and Buckley, J. 2011. Improved Oil Recovery by Low-Salinity Waterflooding. J Pet Technol **63** (5): 106–112. SPE-129421-PA. http://dx.doi.org/10.2118/129421-PA.

Romero-Zeron, L. B., Hum, F. M., and Kantzas, A. 2008. Characterization of Crosslinked Gel Kinetics and Gel Strength by Use of NMR. *SPE Res Eval & Eng* **11** (3): 439–453. SPE-86548-PA. http://dx.doi.org/10.2118/86548-PA.

Schutjens, P. M. T. M., Hausenblas, M., Dijkshorn, M. et al. 1995. The Influence of Intergranular Microcracks on the Petrophysical Properties of Sandstone—Experiments to Quantify Effects of Core Damage. Presented at the International Symposium of the Society of Core Analysts, San Francisco, USA. SCA-9524.

Seright, R. S. 1995. Gel Placement in Fractured Systems. *SPE Prod & Fac* **10** (4): 241–248. SPE-27740-PA. http://dx.doi.org/10.2118/27740-PA.

Seright, R. S. 1999. Polymer Gel Dehydration During Extrusion Through Fractures. *SPE Prod & Fac* **14** (2): 110–116. SPE-56126-PA. http://dx.doi.org/10.2118/56126-PA.

Seright, R. S. 2001. Gel Propagation Through Fractures. *SPE Prod & Fac* **16** (4): 225–231. SPE-74602-PA. http://dx.doi.org/10.2118/74602-PA.

Seright, R. S. 2003a. An Alternative View of Filter-Cake Formation in Fractures Inspired by Cr(III)-Acetate-HPAM Gel Extrusion. *SPE Prod & Fac* **18** (1): 65–72. SPE-81829-PA. http://dx.doi.org/10.2118/81829-PA.

Seright, R. S. 2003b. Washout of Cr(III)-Acetate-HPAM Gels From Fractures. Presented at the International Symposium on Oilfield Chemistry, Houston, USA, 5–7 February. SPE-80200-MS. http://dx.doi.org/10.2118/80200-MS.

Tie, H. 2006. *Oil Recovery by Spontaneous Imbibition and Viscous Displacement From Mixed-Wet Carbonates*. PhD thesis, 238, Department of Chemical and Petroleum Engineering. Laramie, Wyoming, The University of Wyoming.

Tu, T. N. and Wisup, B. 2011. Investigating the Effect of Polymer Gels Swelling Phenomenon Under Reservoir Conditions on Polymer Conformance Control Process. Presented at the International Petroleum Technology Conference, Bangkok, 15–17 November. IPTC-14673-MS. http://dx.doi.org/10.2523/14673-MS.

Uhl, J. T., Ching, T. Y., and Bae, J. H. 1995. A Laboratory Study of New, Surfactant-Containing Polymers for High-Salinity Reservoirs. *SPE Advanced Technology Series* **3** (1): 113–119. SPE-26400-PA. http://dx.doi.org/10.2118/26400-PA.

Vossoughi, S. 2000. Profile Modification Using In Situ Gelation Technology—A Review. *J. Petrol. Sci. & Eng.* **26** (1–4): 199–209. http://dx.doi.org/10.1016/S0920-4105(00)00034-6.

Wilton, R. and Asghari, K. 2007. Improving Gel Performance in Fractures: Chromium Pre-Flush and Overload. *J Can Pet Technol* **46** (2). SPE-07-02-04-PA. http://dx.doi.org/10.2118/07-02-04-PA.

Witherspoon, P. A., Wang, J. S. Y., Iwai, K. et al. 1980. Validity of Cubic Law for Fluid Flow in a Deformable Rock Fracture. *Water Resour. Res.* **16** (6): 1016–1024. http://dx.doi.org/10.1029/WR016i006p01016.

Wu, Y., Mahmoudkhani, A., Watson, P. et al. 2012. Development of New Polymers With Better Performance Under Conditions of High Temperature and High Salinity. Presented at the SPE EOR Conference at Oil and Gas West Asia. Muscat, Oman, 16–18 April. SPE-155653-MS. http://dx.doi.org/10.2118/155653-MS.

Young, T. S., Hunt, J. A., Green, D. W. et al. 1989. Study of Equilibrium Properties of Cr(III)/Polyacrylamide Gels by Swelling Measurement and Equilibrium Dialysis. *SPE Res Eval & Eng* **4** (3): 348–356. SPE-14334-PA. http://dx.doi.org/10.2118/14334-PA.

Zhang, H. and Bai, B. 2011. Preformed-Particle-Gel Transport Through Open Fractures and Its Effect on Water Flow. *SPE J.* **16** (2): 388–400. SPE-129908-PA. http://dx.doi.org/10.2118/129908-PA.

Bergit Brattekås is currently a researcher at the National IOR Centre of Norway. She previously worked at the University of Bergen and as a visiting researcher at the Petroleum Recovery Research Center of New Mexico Tech. Brattekås research interests are EOR and flow mechanisms in mature oil reservoirs (e.g., increasing sweep efficiency by injection of polymer gels or foam). She holds MSc and PhD degrees in reservoir physics from the University of Bergen, Norway.

Arne Graue is professor of physics at the Department of Physics and Technology, University of Bergen, where he is head of the Petroleum and Process Technology Research Group. His scientific interest is within reservoir physics, emphasizing heterogeneous and fractured reservoirs, multiphase flow in porous media, in-situ fluid-saturation imaging, laboratory investigation of integrated EOR techniques, carbon dioxide sequestration, and gas hydrates. Graue has published more than 200 scientific publications and supervised more than 120 PhD and MS degree students. He holds an MS degree in experimental nuclear physics and a PhD degree in reservoir physics, all from the University of Bergen.

Randy Seright is a senior engineer at the Petroleum Recovery Research Center of New Mexico Tech in Socorro, New Mexico, where he worked for the past 28 years. He holds a PhD degree in chemical engineering from the University of Wisconsin (Madison). Seright received the SPE/DOE IOR Pioneer award in 2008 for his work on using polymers and gels to improve oil recovery.